Universitat Autònoma de Barcelona

Dipòsit digital de documents de la UAB

1   **BMP7 overexpression in adipose tissue induces white**

2   **adipogenesis and improves insulin sensitivity in ob/ob mice**

3

4   Estefania Casana[1,2,3*], Veronica Jimenez[1,2,3*], Victor Sacristan[1,2], Sergio

5   Muñoz[1,2,3], Claudia Jambrina[1,2,3], Jordi Rodó[1,2], Miquel Garcia[1,2,3], Cristina

6   Mallol[1,2], Xavier León[1,2,3], Sylvie Franckhauser[1,2,3] and Fatima Bosch[1,2,3#]

7

8   [1]Center of Animal Biotechnology and Gene Therapy (CBATEG), [2]Department of

9   Biochemistry and Molecular Biology, Universitat Autònoma de Barcelona,

10   08193 Bellaterra, and [3]CIBER de Diabetes y Enfermedades Metabólicas

11   Asociadas (CIBERDEM), 28029 Madrid, Spain.

12

13

14   * These authors contributed equally to this work.

15

16   # To whom correspondence should be addressed:

17   Center of Animal Biotechnology and Gene Therapy

18   Edifici H, Universitat Autònoma de Barcelona

19   08193 Bellaterra (Barcelona)

20   SPAIN

21   Tel: +34 93 581 41 82

22   E-mail: fatima.bosch@uab.cat

23

24   **Running title:** BMP7 induces white adipogenesis

ABSTRACT

Background/Objectives: During obesity, hypertrophic enlargement of white adipose tissue (WAT) promotes ectopic lipid deposition and development of insulin resistance. In contrast, WAT hyperplasia is associated with preservation of insulin sensitivity. The complex network of factors that regulate white adipogenesis is not fully understood. Bone morphogenic protein 7 (BMP7) can induce brown adipogenesis, but its role on white adipogenesis remains to be elucidated. Here, we assessed BMP7-mediated effects on white adipogenesis in ob/ob mice.

Methods: BMP7 was overexpressed in either WAT or liver of ob/ob mice using adeno-associated viral (AAV) vectors. Analysis of gene expression, histological and morphometric alterations, and metabolites and hormones concentrations were carried out.

Results: Overexpression of BMP7 in adipocytes of subcutaneous and visceral WAT increased fat mass, the proportion of small-size adipocytes and the expression of adipogenic and mature adipocyte genes, suggesting induction of adipogenesis irrespective of fat depot. These changes were associated with reduced hepatic steatosis and improved insulin sensitivity. In contrast, liver-specific overproduction of BMP7 did not promote WAT hyperplasia despite BMP7 circulating levels were similar to those achieved after genetic engineering of WAT.

Conclusions: This study unravels a new autocrine/paracrine role of BMP7 on white adipogenesis and highlights that BMP7 may modulate WAT plasticity and increase insulin sensitivity.

INTRODUCTION

Obesity and type 2 diabetes (T2D) are strongly associated and have become an alarming growing health problem worldwide. Obesity has been causally linked to the development of insulin resistance, type 2 diabetes (T2D), arthritis, cancer, cardiovascular diseases and Alzheimer's disease. These obesity-linked complications lead to reduced life expectancy and poor quality of life, thus representing a massive burden for the health-care systems.

Obesity is a condition where adipose tissue mass is increased due to an imbalance between energy intake and expenditure. Expandability of white adipose tissue (WAT) may result from an increase in the size (hypertrophy) and/or in the number of adipocytes (hyperplasia), by the differentiation of new adipocytes from undifferentiated preadipocytes (adipogenesis) [1–3]. Adipocyte hypertrophy is closely linked to adipose dysfunction and inflammation, abnormal secretion patterns of adipokines, ectopic lipid deposition in non-adipose tissues such as liver, skeletal muscle and heart, and whole-body insulin resistance and T2D, not only in obese but also in lean individuals [4,5]. Conversely, WAT expansion through hyperplasia has been associated with improved insulin sensitivity [6–8].

Under physiological conditions, in a situation of positive energy balance, in both humans and rodents excess lipids is stored primarily via hyperplasia in the subcutaneous adipose tissue (SAT), since this depot has greater adipogenic differentiation capacity than visceral adipose tissue (VAT) [4,9,10]. In obesity, recruitment and adipogenic differentiation of the stromal vascular precursor cells in SAT are impaired. Therefore, subcutaneous adipocytes become

75   hypertrophic and adipogenesis is restricted to VAT, which ultimately also

76   expands through hypertrophy when its hyperplasic capacity is exceeded [4,11–

77   17]. Enhancement of WAT hyperplasia may limit the deleterious metabolic

78   effects mediated by dysfunctional white adipocytes and help to preclude hepatic

79   steatosis and insulin resistance. Nevertheless, the complex network of factors

80   that regulate white adipogenesis has not been fully elucidated.

81   The bone morphogenetic protein (BMP) family belongs to the

82   transforming growth factor β (TGFβ) superfamily of cytokines that regulate an

83   array of fundamental cellular processes, including proliferation, differentiation,

84   apoptosis and morphogenesis [18]. BMPs play major roles in adipogenesis, not

85   only regulating progenitor cell determination, but also promoting terminal

86   adipogenic differentiation [19,20]. Among them, BMP7 was considered to be

87   essential for brown adipogenesis in both committed brown preadipocytes and

88   uncommitted multipotent mesenchymal precursors [19,21]. In contrast, BMP2

89   and BMP4 had been described as master regulatory factors that drive the

90   commitment and differentiation of adipocyte precursors into white adipocytes

91   [19]. Recent studies have evidenced that BMP2 and BMP4, as well as BMP9

92   and BMP14, can trigger both white and brown adipogenesis [20,22–30].

93   Nevertheless, whether the brown adipogenic factor BMP7 may also induce

94   white adipogenesis is unknown.

95   In this study, specific overexpression of BMP7 in WAT of adult obese

96   mice resulted in redistribution of the size of white adipocytes, with a greater

97   proportion of small-size adipocytes both in SAT and VAT, and amelioration of

98   insulin resistance. In contrast, overexpression of BMP7 in the liver led to similar

99   levels of circulating BMP7 but did not promote WAT hyperplasia. These results

4

100   are consistent with a paracrine/autocrine role of BMP7 inducing white

101   adipogenesis.

102

1. MATERIAL AND METHODS

2.1. Animals. Eleven-week-old B6.V-*Lep^ob*/OlaHsd (ob/ob) male mice were used. Mice were kept in a specific pathogen-free facility (SER-CBATEG, UAB) and maintained under a light-dark cycle of 12 h at 22 ºC. Mice were fed *ad libitum* with a standard diet (2018S Teklad Global Diets®, Envigo). For tissue sampling, mice were anesthetized with inhalational anesthetic isoflurane (IsoFlo®, Abbott Laboratories, Abbott Park, IL, US) and sacrificed. Tissues of interest were excised and kept at -80°C or in formalin until analysis. Animal care and experimental procedures were approved by the Ethics Committee in Animal and Human Experimentation of the Universitat Autònoma de Barcelona.

2.2. Recombinant AAV vectors. AAV expression cassettes were obtained by cloning, between the ITRs of AAV2, a murine optimized BMP7 coding-sequence (moBMP7) under the control of either: i) the liver-specific human α1-antitrypsin promoter (hAAT) (AAV-hAAT-BMP7); or ii) the ubiquitous early CMV enhancer/chicken beta actin promoter (CAG) with the addition of 4 tandem repeats of miRT122a sequence (5'CAAACACCATTGTCACACTCCA3') and miRT1 sequence (5'TTACATACTTCTTTACATTCCA3') in the 3' untranslated region of the expression cassette. The moBMP7 sequence comprised in the expression cassettes was a murine BMP7 coding-sequence that was codon-optimized to enhance production of wild-type BMP7 protein using the GeneOptimizer algorithm (GeneArt; Life Technologies), which relies on a multifactorial approach. Non-coding cassettes, carrying either the hAAT or the CAG promoter but no transgene, were used to produce null vectors. Single-

6

stranded AAV vectors of serotype 8 were produced by triple transfection in HEK293 cells. HEK293 cells were kindly provided by K.A. High, Children's Hospital of Philadelphia. AAV vectors were purified using an optimized CsCl gradient–based purification protocol that renders vector preps of high purity and devoid of empty capsids [31]. Viral vectors were determined by fluorescence using the Quant-iT™ PicoGreen™ dsDNA Assay Kit (Invitrogen). A phage lambda DNA was used as standard curve to calculate the titer of viral vectors.

2.3. Administration of AAV vectors. Systemic intravenous and intra-epididimal WAT (eWAT) administration of AAV vectors were performed as previously described [32,33].

2.4. Immunohistochemistry. Tissues were fixed for 12-24 h in 10% formalin, embedded in paraffin and sectioned. Sections were incubated overnight at 4ºC with rat anti-Mac2 antibody (CL8942AP; Cedarlane). Biotinylated rabbit anti-rat (E0467; Dako) was used as secondary antibody. The ABC peroxidase kit (Pierce) was used for immunodetection, and sections were counterstained in Mayer's hematoxylin. Morphometric analysis of adipocyte size was performed in WAT sections stained with hematoxylin–eosin as previously described [34]. A minimum of four animals per group was used and at least 250 adipocytes per animal were analyzed.

2.5. RNA analysis. Total RNA was obtained from different tissues using isolation reagent (Tripure, Roche, for liver samples and QIAzol, Qiagen, for adipose depots) and a RNeasy Minikit (Qiagen) and treated with DNAseI

(Qiagen). One µg of RNA was reverse-transcribed using the Transcriptor First Strand cDNA Synthesis kit (Roche). Real-time quantitative PCR (qRT-PCR) was performed in a LightCycler (Roche) using 1) the LightCycler 480 SYBR Green I Master Mix (Roche) and murine primers (Table S1) or 2) the LightCycler 480 Probes Master Mix (Roche) and murine primers and probes (IDT, Leuven, Germany) (Table S2). Data were normalized to *Rplp0* expression.

2.6. Hormone and metabolite assays. Hepatic triglyceride content was determined after chloroform:methanol (2:1 vol/vol) extraction of total lipids, as previously described [35]. Triglycerides were quantified spectrophotometrically using an enzymatic assay (Horiba-ABX) in a Pentra 400 Analyzer (Horiba-ABX). Glycemia was determined using a Glucometer Elite^{TM} (Bayer) and insulin levels were measured using the Rat Insulin ELISA kit (90010, Crystal Chem). Serum BMP7 and adiponectin levels were determined using the Human BMP7 ELISA kit (DBP700, R&D Systems) and the Mouse Adiponectin ELISA kit (80569, Crystal Chem).

2.7. Insulin tolerance test. Insulin (Humulin Regular; Eli Lilly) was injected intraperitoneally at a dose of 0.75 IU/kg body weight to fed mice. Glycemia was measured in blood samples from tail vein at the indicated time points.

2.8. Indirect calorimetry and activity. An indirect open circuit calorimeter (Oxylet, Panlab) was used to monitor O_2 consumption, CO_2 production and activity. Mice were individualized and acclimated to the metabolic chambers for 24h. O_2 consumption and CO_2 production data were collected in each cage for 3

178 min, every 15 min, for 24 h during the light and dark cycles and adjusted by

179 body weight. Activity was recorded continuously for 24 h during the light and

180 dark cycles.

181

182 **2.9. Statistical analysis.** Sample size determination was based on previous

183 experience with similar studies. Mice were randomly divided into groups (n=8-

184 10 per group). In addition, we tested that the mean body weight and the mean

185 glycemia were statistically not different for each experimental group prior to

186 assignment to treatment groups. Furthermore, each experimental group was

187 caged separately to avoid any caging effects. All tests and analyses were

188 performed by investigators blinded to the treatment. All results are expressed as

189 mean ± SEM. Values higher than 1.5IQR were considered atypical and were

190 excluded from analyses. Differences between groups were compared by two-

191 sided Student's *t*-test. Statistical significance was considered if *P*< 0.05.

192

3. RESULTS

3.1. BMP7 promotes white adipose tissue expansion

Intra-adipose depot delivery of AAV8 vectors in both lean and obese diabetic mice leads to long-term efficient transduction of WAT and is a useful tool to study adipose pathophysiology and adipocyte function [32,33,36]. To examine the role of BMP7 on white adipogenesis, we chose ob/ob mice as a well-established model of obesity with WAT hypertrophy, insulin resistance and a significant accumulation of hepatic triglycerides relatively early in life [37,38]. A cohort of ob/ob mice received an intra-epidydimal WAT (eWAT) injection of 1×10^{12} vg/mouse of AAV8 vectors encoding murine BMP7 under the transcriptional control of the ubiquitous CAG promoter. To avoid expression of the transgene in other main organs for which AAV8 shows strong tropism, such as liver and heart [39–41], we took advantage of microRNAs (miRs). Target sequences for miR-122a and miR-1, which selectively de-target transgene expression from liver and heart when included into AAV vectors [32,42], were added in tandem repeats of four copies to the 3'-UTR of the murine BMP7 expression cassette (AAV8-CAG-BMP7-miRT122-miRT1; AAV-BMP7). Another cohort of ob/ob mice administered with 1×10^{12} vg of non-coding null vectors (AAV8-null) served as controls.

Animals treated intra-eWAT with AAV-BMP7 vectors showed high BMP7 overexpression mainly in this depot but also in retroperitoneal (rWAT), mesenteric (mWAT) and inguinal (iWAT) depots (Figure 1A), as previously reported [33]. Marginal BMP7 expression was detected in iBAT (Figure 1A). As expected, microRNA target sequences efficiently prevented BMP7 expression

10

218 in the liver (Figure 1A) and heart (data not shown). In agreement with previous

219 reports demonstrating the high secretory capacity of AAV-modified WAT

220 [32,33], increased BMP7 circulating levels were observed in mice receiving

221 AAV-BMP7 vectors (Figure 1B).

222   As animals aged, ob/ob mice overexpressing BMP7 in white adipocytes

223 showed increased body weight compared with AAV-null-treated counterparts

224 (Figure 1C) although no differences in food intake were observed (Figure S1A).

225 A tendency towards a decrease in spontaneous activity during the dark phase

226 may have contributed to body weight gain (Figure S1B). Treatment with AAV-

227 BMP7 vectors also led to a specific increase of the main WAT depots weight

228 (Figure 1D). This was parallel to a redistribution of the size of white adipocytes,

229 with a greater proportion of small-size adipocytes in both eWAT and iWAT

230 (Figure 1E,F and Figure S1C). Altogether, these observations suggested that

231 BMP7 induced white adipogenesis, irrespective of fad pad.

232

233 **3.2. BMP7 induces expression of adipogenic markers and decreases**

234   **WAT inflammation**

235 The expression of the preadipocyte marker Preadipocyte factor 1 (*Pref1*) as well

236 as that of the final adipogenic inducers Peroxisome Proliferator Activated

237 Receptor Gamma (*Pparγ*) and CCAAT/enhancer binding protein alpha *(Cebpα)*

238 was induced in eWAT and iWAT of ob/ob mice overexpressing BMP7 in white

239 adipocytes (Figure 2A,B). These results suggested induction of white

240 adipogenesis in SAT and VAT of these animals. In addition, the expression of

241 proteins involved in lipid accumulation, which are markers of mature adipocytes,

242 such as sterol regulatory element binding transcription factor 1 (*Srebf1*), fatty

243　acid synthase (*Fasn*), acetyl-CoA carboxylase 1 (*Acc1*), acetyl-CoA carboxylase

244　2 (*Acc2*), fatty acid-binding protein 4 (Fabp4), perilipin 1 (Plin1) and glucose

245　transporter type 4 (Slc2a4), was also increased in eWAT and iWAT of AAV-

246　BMP7-treated animals (Figure 2C,D).

247　　　In agreement with expansion of WAT, ob/ob mice overexpressing BMP7

248　showed increased adiponectin levels (Figure 2E). WAT inflammation was also

249　decreased in these mice, evidenced by lower presence of macrophages,

250　revealed as "crown-like" structures, and reduced expression of the macrophage

251　markers *F480* and *Cd68* and of the pro-inflammatory cytokines *Mcp1* and *Tnfα*

252　compared with AAV-null treated mice (Figure 2F-I).

253

254　**3.3.　BMP7 overexpression in WAT does not induce brown adipogenesis**

255　In contrast to the observations made in WAT, ob/ob mice treated with AAV-

256　BMP7 or AAV-null showed similar iBAT weight and lipid deposition in this depot

257　(Figure 1D and Figure 3A) likely due to the marginal expression of BMP7 in

258　BAT (Figure 1A). BMP7 can induce brown adipocyte differentiation *in vitro* and

259　non-shivering thermogenesis [21,43]. However, no differences in the expression

260　of pro-adipogenic and mature adipocyte markers were observed in iBAT of

261　AAV-BMP7-treated mice (Figure 3B,C). Moreover, multilocular beige adipocytes

262　were not detected in iWAT (Figure 1E) and the expression of the thermogenic

263　markers uncoupling protein 1 (Ucp1) and peroxisome proliferator-activated

264　receptor gamma coactivator 1-alpha (*Ppargc1a*) remained unchanged in iBAT

265　and iWAT (Figure 3D,E). Consistent with these findings, WAT-derived BMP7

266　failed to induce energy expenditure (Figure 3F).

267

268 **3.4. BMP7 overproduction in WAT ameliorates hepatic steatosis and**
269 **improves insulin resistance**

270 Histological analysis of the liver revealed that null-treated ob/ob mice developed

271 marked hepatic steatosis (Figure 4A). In contrast, hepatic lipid deposition was

272 decreased in ob/ob mice overexpressing BMP7 in WAT (Figure 4A,B). This was

273 parallel to reduced hepatic inflammation, evidenced by decreased number of

274 Mac2$^+$ cells (Figure 4C) and lower liver expression of *Cd68* (Figure 4D).

275 Ob/ob mice treated with AAV-null vectors showed normal fed glycaemia

276 but were hyperinsulinemic (Figure 5A,B). In contrast, ob/ob mice treated with

277 BMP7 were normoglycemic and presented a marked reduction of serum insulin

278 levels (Figure 5A,B), suggesting improved insulin sensitivity. The intraperitoneal

279 insulin tolerance test (ITT) confirmed amelioration of insulin resistance in AAV-

280 BMP7-treated ob/ob mice (Figure 5C).

281

282 **3.5. BMP7 overexpression in the liver does not induce white**
283 **adipogenesis**

284 To elucidate whether the BMP7-mediated induction of WAT hyperplasia was

285 due to the paracrine/autocrine action of BMP7 in WAT or to the increased

286 circulating levels of the factor, the liver of ob/ob mice was genetically

287 engineered to overproduce BMP7. To this end, ob/ob mice were administered

288 intravenously (IV) with 5×10^{11} vg of AAV8 vectors encoding murine BMP7 under

289 the control of the liver-specific hAAT promoter (AAV-hAAT-BMP7). As controls,

290 another cohort of ob/ob mice received the same dose of non-coding null vectors

291 (AAV-hAAT-null).

292   Ob/ob mice treated with AAV-hAAT-BMP7 vectors showed specific

293   hepatic overexpression of BMP7 (Figure 6A). This led to increased BMP7

294   circulating levels (Figure 6B), which were similar to those observed in ob/ob

295   mice overexpressing BMP7 in white adipocytes (Figure 1B). However, body

296   weight of ob/ob mice overproducing BMP7 in the liver was indistinguishable

297   from that of AAV-hAAT-null-treated mice (Figure 6C). In addition, the weight of

298   liver and adipose depots was similar in both groups of animals (Figure 6D).

299   Moreover, white adipocyte size of ob/ob treated with AAV-hAAT-BMP7 vectors

300   remained unchanged (Figure 6E and Figure S2A,B). In agreement, the

301   expression of genes involved in adipogenesis and of markers of mature

302   adipocytes (*Pref1*, *Wnt10b*, *Cebpß*, *Pparγ*, *Cebpα, Fabp4*, *Plin1*, *Slc2a4)* was

303   similar between BMP7 and null-treated ob/ob mice in both eWAT and iWAT

304   (Figure 6F and Figure S2C). These results suggested that BMP7-mediated

305   effects in white adipogenesis likely resulted from autocrine/paracrine effects of

306   BMP7 in WAT.

307   According to the lack of hyperplasic expansion of WAT, both adiponectin

308   levels and the degree of WAT inflammation remained unchanged in ob/ob mice

309   overexpressing BMP7 in the liver compared with control mice (Figure 6G-I).

310   In addition, no differences in lipid deposition or in the expression levels of

311   the adipogenic and mature adipocyte markers *Pref1*, *Pparγ*, *Cebpα*, *Prdm16,*

312   *Fabp4 and Plin* (Figure S2D,E) were observed in iBAT of AAV-hAAT-BMP7-

313   treated mice. Multilocular adipocytes were neither detected in iWAT of these

314   mice (Supplementary Figure 2B) and the expression of the thermogenic

315   markers *Ucp1* and *Ppargc1a* remained unchanged in iWAT and iBAT (Figure

316   S2F,G).

14

317   Moreover, similar hepatic lipid deposition, TG content or inflammation
318   were detected in AAV-hAAT-BMP7-treated mice compared with null-treated
319   ob/ob mice (Figures 6H and 6J,K and Figure S2H), indicating lack of
320   amelioration of hepatosteatosis. In agreement, animals treated with AAV-hAAT-
321   BMP7 or AAV-null vectors showed similar glycemia and hyperinsulinemia
322   (Figure 6L,M).
323

4. DISCUSSION

The results reported in this study suggest that BMP7 is able to induce white adipogenesis *in vivo*. Enhanced expression of adipogenic genes increased both adiposity and the proportion of small-size adipocytes in subcutaneous and visceral WAT depots of ob/ob mice in which BMP7 was overexpressed. In contrast, when BMP7 was overproduced in the liver, no changes in fat mass, adipocyte size distribution or expression levels of adipogenic markers were observed despite similar BMP7 circulating levels. This was consistent with BMP7-mediated induction of hyperplasic expansion of WAT in an autocrine/paracrine manner. Compared with the low BMP7 circulating levels reached in this study after engineering WAT or liver with AAV-BMP7 vectors (approximately 350 or 550 pg/ml, respectively), short-term treatment with adenoviral vectors overexpressing BMP7 resulted in very high serum concentration of the factor [21,44]. In these studies, serum levels of BMP7 in the first publication ranged 3000-4000 pg/ml [21] and several hundred-fold higher in the second one [44]. Such very high levels of BMP7 decreased fat mass, increased energy expenditure and attenuated hyperglycemia and obesity [21,44], suggesting that BMP7 may elicit different effects depending on the circulating levels.

Despite an increase in body weight and fat mass, obese ob/ob mice overexpressing BMP7 in WAT presented reduced hepatic steatosis, WAT and liver inflammation, and increased insulin sensitivity, together with increased proportion of small-size adipocytes. Although the absolute number of new adipocytes was not quantified in SAT and VAT, our results showed an

16

349 increased proportion of smaller adipocytes in BMP7-treated mice together with

350 increased expression of adipogenic markers, suggesting hyperplasia in both

351 WAT depots. These results suggested that BMP7 was able to shift the

352 unhealthy obese phenotype of ob/ob mice towards an improved metabolic

353 phenotype. It has been observed that a subset of obese humans can also

354 develop metabolically healthy obesity [45], with reduced hepatic fat deposition

355 and increased insulin sensitivity despite high BMI [46,47].

356 Similar to the observations made in ob/ob mice overexpressing BMP7 in

357 WAT, hyperplasic expansion of SAT and improved insulin sensitivity is also

358 observed in several animal models, such as ob/ob mice overexpressing

359 mitoNEET (a mitochondrial membrane protein) in adipose tissue [48]; HFD-fed

360 mice treated with adipogenic cocktails [49], or FGF21 knock-out mice treated

361 with recombinant FGF21 [8]. Moreover, treatment of obese insulin-resistance

362 patients with pioglitazone increases WAT adipogenesis, particularly in SAT [7].

363 However, our results suggest that not only subcutaneous but also visceral

364 adipose hyperplasia may be responsible for the metabolic benefit induced by

365 BMP7. In agreement, obese mouse models displaying VAT hyperplasia, such

366 as transgenic mice overexpressing GLUT4 in adipose tissue [50], ob/ob mice

367 lacking the liver X receptors α and β (LXRαβ) [51], or transgenic mice

368 overexpressing CIDEA in adipose tissue [52], also show improved glucose

369 homeostasis and reduced hepatic steatosis.

370 Increased circulating adiponectin levels in ob/ob mice overexpressing

371 BMP7 in white adipocytes may also contribute to improve insulin sensitivity.

372 Adiponectin production is closely linked to adipose tissue hyperplasia, as

373 indicated by previous reports [8,53,54]. Transgenic mice overexpressing

374 adiponectin in adipose tissue presented increased fat mass, WAT hyperplasia

375 and improved insulin sensitivity [37]. Furthermore, the induction of SAT and/or

376 VAT hyperplasia observed in the previously mentioned animal models led to

377 increased plasma adiponectin levels [8,48,51,52]. Likewise, T2D patients

378 treated with TZD show increased plasma adiponectin concentration [55].

379 Adiponectin also has insulin-sensitizing and anti-inflammatory properties and is

380 additionally associated with decreased hepatic steatosis [37,56,57]. In humans,

381 adiponectin levels are inversely correlated with development of non-alcoholic

382 fatty liver disease and with the degree of insulin resistance and T2D [58,59].

383 Treatment of mice or rats fed a high fat diet (HFD) with recombinant adiponectin

384 decreased liver steatosis and increased insulin sensitivity [60,61]. Similarly,

385 muscular or hepatic gene transfer of adiponectin using AAV vectors enhanced

386 insulin sensitivity and reduced inflammation and hepatic lipid deposition in HFD-

387 fed diabetic rats [56,57]. Moreover, decreased inflammation and hepatic lipid

388 deposition were observed in animal models that develop WAT hyperplasia and

389 showed increased adiponectin levels [37,48,51]. All these results suggest that

390 the increased circulating adiponectin levels observed in ob/ob mice

391 overexpressing BMP7 in white adipocytes may play an important role in the

392 amelioration of liver and WAT inflammation, thus contributing to reduce pro-

393 inflammatory immune cells and cytokine production, as well as, liver steatosis.

394 These phenotypic benefits together with increased WAT hyperplasia would in

395 turn improve the insulin sensitivity observed in these ob/ob mice. However,

396 given that the ob/ob model is deficient in leptin, it would be of particular interest

397 to study whether a similar BMP7-mediated metabolic benefit would be also

398 obtained in dietary mouse models of obesity.

399   Altogether, our study unravels for the first time a new autocrine/paracrine

400   role of BMP7 on white adipogenesis and highlights that BMP7, when locally

401   expressed in WAT may be a good candidate to modulate adipose tissue

402   plasticity in order to reduce obesity-associated fatty liver and insulin resistance.

403

AUTHOR CONTRIBUTIONS

EC, VJ and FB designed and supervised experiments and analyzed data. EC, VJ, VS, SM, CJ, JR, MG and CM generated reagents and performed experiments. XL produced AAV vectors. EC, VJ, SF, and FB, contributed to discussion, and wrote the manuscript.

COMPETING INTERESTS

The authors declare no competing interests.

Supplementary information is available at International Journal of Obesity's website.

REFERENCES

430

431   1.   Wang QA, Tao C, Gupta RK, Scherer PE (2013) Tracking adipogenesis during

432   white adipose tissue development, expansion and regeneration. *Nat Med* **19**:

433   1338–1344.

434   2.   Spalding KL, Arner E, Westermark PO, Bernard S, Buchholz BA, Bergmann O,

435   Blomqvist L, Hoffstedt J, Näslund E, Britton T, et al. (2008) Dynamics of fat cell

436   turnover in humans. *Nature* **453**: 783–787.

437   3.   Arner P, Andersson DP, Thörne A, Wirén M, Hoffstedt J, Näslund E, Thorell A,

438   Rydén M (2013) Variations in the Size of the Major Omentum Are Primarily

439   Determined by Fat Cell Number. *J Clin Endocrinol Metab* **98**: E897–E901.

440   4.   Hammarstedt A, Gogg S, Hedjazifar S, Nerstedt A, Smith U (2018) Impaired

441   adipogenesis and dysfunctional adipose tissue in human hypertrophic obesity.

442   *Physiol Rev* **98**: 1911–1941.

443   5.   Acosta JR, Douagi I, Andersson DP, Bäckdahl J, Rydén M, Arner P,

444   Laurencikiene J (2016) Increased fat cell size: a major phenotype of

445   subcutaneous white adipose tissue in non-obese individuals with type 2

446   diabetes. *Diabetologia* **59**: 560–570.

447   6.   Hoffstedt J, Arner E, Wahrenberg H, Andersson DP, Qvisth V, Löfgren P, Rydén

448   M, Thörne A, Wirén M, Palmér M, et al. (2010) Regional impact of adipose tissue

449   morphology on the metabolic profile in morbid obesity. *Diabetologia* **53**: 2496–

450   2503.

451   7.   McLaughlin TM, Liu T, Yee G, Abbasi F, Lamendola C, Reaven GM, Tsao P,

452   Cushman SW, Sherman A (2010) Pioglitazone increases the proportion of small

453   cells in human abdominal subcutaneous adipose tissue. *Obesity (Silver Spring)*

454   **18**: 926–931.

455   8.   Li H, Wu G, Fang Q, Zhang M, Hui X, Sheng B, Wu L, Bao Y, Li P, Xu A, et al.

456   (2018) Fibroblast growth factor 21 increases insulin sensitivity through specific

457   expansion of subcutaneous fat. *Nat Commun* **9**: 272.

458   9.   Fried SK, Lee M-J, Karastergiou K (2015) Shaping fat distribution: New insights

459   into the molecular determinants of depot- and sex-dependent adipose biology.

460   *Obesity (Silver Spring)* **23**: 1345–1352.

461   10.   Carobbio S, Pellegrinelli V, Vidal-Puig A (2017) Adipose Tissue Function and

462   Expandability as Determinants of Lipotoxicity and the Metabolic Syndrome. *Adv*

463   *Exp Med Biol* **960**: 161–196.

464   11.   Wang QA, Tao C, Gupta RK, Scherer PE (2013) Tracking adipogenesis during

465   white adipose tissue development, expansion and regeneration. *Nat Med* **19**:

466   1338–1344.

467   12.   Kim SM, Lun M, Wang M, Senyo SE, Guillermier C, Patwari P, Steinhauser ML

468   (2014) Loss of white adipose hyperplastic potential is associated with enhanced

469   susceptibility to insulin resistance. *Cell Metab* **20**: 1049–1058.

470   13.   Jeffery E, Church CD, Holtrup B, Colman L, Rodeheffer MS (2015) Rapid depot-

471   specific activation of adipocyte precursor cells at the onset of obesity. *Nat Cell*

472   *Biol* **17**: 376–385.

473   14.   Permana PA, Nair S, Lee Y-H, Luczy-Bachman G, Vozarova De Courten B,

474   Tataranni PA (2004) Subcutaneous abdominal preadipocyte differentiation in

475   vitro inversely correlates with central obesity. *Am J Physiol Endocrinol Metab*

476   **286**: E958-62.

477   15.   Tchoukalova Y, Koutsari C, Jensen M (2007) Committed subcutaneous

478   preadipocytes are reduced in human obesity. *Diabetologia* **50**: 151–157.

479   16.   Almuraikhy S, Kafienah W, Bashah M, Diboun I, Jaganjac M, Al-Khelaifi F,

480   Abdesselem H, Mazloum NA, Alsayrafi M, Mohamed-Ali V, et al. (2016)

481   Interleukin-6 induces impairment in human subcutaneous adipogenesis in

482   obesity-associated insulin resistance. *Diabetologia* **59**: 2406–2416.

483   17.   Arner P, Arner E, Hammarstedt A, Smith U (2011) Genetic predisposition for

484   type 2 diabetes, but not for overweight/obesity, is associated with a restricted

485   adipogenesis. *PLoS One* **6**: e18284.

486   18.   Carreira ACO, Zambuzzi WF, Rossi MC, Filho RA, Sogayar MC, Granjeiro JM

487   (2015) Bone Morphogenetic Proteins: Promising Molecules for Bone Healing,

488   Bioengineering, and Regenerative Medicine. In, *Vitamins and Hormones* pp

489   293–322.

490   19.   Schulz TJ, Tseng YH (2009) Emerging role of bone morphogenetic proteins in

491   adipogenesis and energy metabolism. *Cytokine Growth Factor Rev* **20**: 523–

492   531.

493   20.   Blázquez-Medela AM, Jumabay M, Rajbhandari P, Sallam T, Guo Y, Yao J,

494   Vergnes L, Reue K, Zhang L, Yao Y, et al. (2019) Noggin depletion in adipocytes

495   promotes obesity in mice. *Mol Metab* **25**: 50–63.

496   21.   Tseng Y-H, Kokkotou E, Schulz TJ, Huang TL, Winnay JN, Taniguchi CM, Tran

497   TT, Suzuki R, Espinoza DO, Yamamoto Y, et al. (2008) New role of bone

498   morphogenetic protein 7 in brown adipogenesis and energy expenditure. *Nature*

499   **454**: 1000–1004.

500   22.   Salisbury EA, Lazard ZW, Ubogu EE, Davis AR, Olmsted-Davis EA (2012)

501   Transient brown adipocyte-like cells derive from peripheral nerve progenitors in

502   response to bone morphogenetic protein 2. *Stem Cells Transl Med* **1**: 874–885.

503   23.   Qian S-W, Tang Y, Li X, Liu Y, Zhang Y-Y, Huang H-Y, Xue R-D, Yu H-Y, Guo

504   L, Gao H-D, et al. (2013) BMP4-mediated brown fat-like changes in white

505   adipose tissue alter glucose and energy homeostasis. *Proc Natl Acad Sci U S A*

506   **110**: E798-807.

507   24.   Kim M, Kim JI, Kim JB, Choe S (2017) The activin-βA/BMP-2 chimera AB204 is

508   a strong stimulator of adipogenesis. *J Tissue Eng Regen Med* **11**: 1524–1531.

509   25.   Gustafson B, Hedjazifar S, Gogg S, Hammarstedt A, Smith U (2015) Insulin

510   resistance and impaired adipogenesis. *Trends Endocrinol Metab* **26**: 193–200.

511   26.   Elsen M, Raschke S, Tennagels N, Schwahn U, Jelenik T, Roden M, Romacho

512   T, Eckel J (2014) BMP4 and BMP7 induce the white-to-brown transition of

513 primary human adipose stem cells. *Am J Physiol Cell Physiol* **306**: C431-40.

514 27. Hinoi E, Nakamura Y, Takada S, Fujita H, Iezaki T, Hashizume S, Takahashi S,

515 Odaka Y, Watanabe T, Yoneda Y (2014) Growth differentiation factor-5

516 promotes brown adipogenesis in systemic energy expenditure. *Diabetes* **63**:

517 162–175.

518 28. Lord E, Bergeron E, Senta H, Park H, Faucheux N (2010) Effect of BMP-9 and

519 its derived peptide on the differentiation of human white preadipocytes. *Growth*

520 *Factors* **28**: 149–156.

521 29. Pei Z, Yang Y, Kiess W, Sun C, Luo F (2014) Dynamic profile and adipogenic

522 role of growth differentiation factor 5 (GDF5) in the differentiation of 3T3-L1

523 preadipocytes. *Arch Biochem Biophys* **560**: 27–35.

524 30. Kuo MM-C, Kim S, Tseng C-Y, Jeon Y-H, Choe S, Lee DK (2014) BMP-9 as a

525 potent brown adipogenic inducer with anti-obesity capacity. *Biomaterials* **35**:

526 3172–3179.

527 31. Ayuso E, Mingozzi F, Montane J, Leon X, Anguela XM, Haurigot V, Edmonson S

528 a, Africa L, Zhou S, High K a, et al. (2010) High AAV vector purity results in

529 serotype- and tissue-independent enhancement of transduction efficiency. *Gene*

530 *Ther* **17**: 503–510.

531 32. Jimenez V, Muñoz S, Casana E, Mallol C, Elias I, Jambrina C, Ribera A, Ferre

532 T, Franckhauser S, Bosch F (2013) In vivo AAV-mediated Genetic Engineering

533 of White and Brown Adipose Tissue in Adult Mice. *Diabetes* **62**: 1–12.

534 33. Jimenez V, Jambrina C, Casana E, Sacristan V, Muñoz S, Darriba S, Rodó J,

535 Mallol C, Garcia M, León X, et al. (2018) FGF21 gene therapy as treatment for

536 obesity and insulin resistance. *EMBO Mol Med* **10**:.

537 34. Muñoz S, Franckhauser S, Elias I, Ferré T, Hidalgo A, Monteys AM, Molas M,

538 Cerdán S, Pujol A, Ruberte J, et al. (2010) Chronically increased glucose uptake

539 by adipose tissue leads to lactate production and improved insulin sensitivity

540 rather than obesity in the mouse. *Diabetologia* **53**: 2417–2430.

24

541 35. Carr TP, Andresen CJ, Rudel LL (1993) Enzymatic determination of triglyceride,

542   free cholesterol, and total cholesterol in tissue lipid extracts. *Clin Biochem* **26**:

543   39–42.

544 36. Lagarrigue S, Lopez-Mejia IC, Denechaud P-D, Escoté X, Castillo-Armengol J,

545   Jimenez V, Chavey C, Giralt A, Lai Q, Zhang L, et al. (2016) CDK4 is an

546   essential insulin effector in adipocytes. *J Clin Invest* **126**: 335–348.

547 37. Kim JY, Van De Wall E, Laplante M, Azzara A, Trujillo ME, Hofmann SM,

548   Schraw T, Durand JL, Li H, Li G, et al. (2007) Obesity-associated improvements

549   in metabolic profile through expansion of adipose tissue. *J Clin Invest* **117**:

550   2621–2637.

551 38. Lindström P (2007) The physiology of obese-hyperglycemic mice [ob/ob mice].

552   *ScientificWorldJournal* **7**: 666–685.

553 39. Gao G-P, Alvira MR, Wang L, Calcedo R, Johnston J, Wilson JM (2002) Novel

554   adeno-associated viruses from rhesus monkeys as vectors for human gene

555   therapy. *Proc Natl Acad Sci U S A* **99**: 11854–11859.

556 40. Zincarelli C, Soltys S, Rengo G, Rabinowitz JE (2008) Analysis of AAV

557   serotypes 1-9 mediated gene expression and tropism in mice after systemic

558   injection. *Mol Ther* **16**: 1073–1080.

559 41. Wang L, Wang H, Bell P, McCarter RJ, He J, Calcedo R, Vandenberghe LH,

560   Morizono H, Batshaw ML, Wilson JM (2010) Systematic Evaluation of AAV

561   Vectors for Liver directed Gene Transfer in Murine Models. *Mol Ther* **18**: 118–

562   125.

563 42. Mallol C, Casana E, Jimenez V, Casellas A, Haurigot V, Jambrina C, Sacristan

564   V, Morró M, Agudo J, Vilà L, et al. (2017) AAV-mediated pancreatic

565   overexpression of Igf1 counteracts progression to autoimmune diabetes in mice.

566   *Mol Metab* **6**: 664–680.

567 43. Schulz TJ, Huang TL, Tran TT, Zhang H, Townsend KL, Shadrach JL, Cerletti

568   M, McDougall LE, Giorgadze N, Tchkonia T, et al. (2011) Identification of

569   inducible brown adipocyte progenitors residing in skeletal muscle and white fat.

570   *Proc Natl Acad Sci U S A* **108**: 143–148.

571 44.   Townsend KL, Suzuki R, Huang TL, Jing E, Schulz TJ, Lee K, Taniguchi CM,

572   Espinoza DO, McDougall LE, Zhang H, et al. (2012) Bone morphogenetic

573   protein 7 (BMP7) reverses obesity and regulates appetite through a central

574   mTOR pathway. *FASEB J* **7**: 1–10.

575 45.   Häring H-U (2016) Novel phenotypes of prediabetes? *Diabetologia* **59**: 1806–

576   1818.

577 46.   Stefan N, Kantartzis K, Machann J, Schick F, Thamer C, Rittig K, Balletshofer B,

578   Machicao F, Fritsche A, Häring H-U (2008) Identification and characterization of

579   metabolically benign obesity in humans. *Arch Intern Med* **168**: 1609–1616.

580 47.   Stefan N, Häring H-U, Schulze MB (2018) Metabolically healthy obesity: the low-

581   hanging fruit in obesity treatment? *lancet Diabetes Endocrinol* **6**: 249–258.

582 48.   Kusminski CM, Holland WL, Sun K, Park J, Spurgin SB, Lin Y, Askew GR,

583   Simcox JA, McClain DA, Li C, et al. (2012) MitoNEET-driven alterations in

584   adipocyte mitochondrial activity reveal a crucial adaptive process that preserves

585   insulin sensitivity in obesity. *Nat Med* **18**: 1539–1549.

586 49.   Lu Q, Li M, Zou Y, Cao T (2014) Induction of adipocyte hyperplasia in

587   subcutaneous fat depot alleviated type 2 diabetes symptoms in obese mice.

588   *Obesity (Silver Spring)* **22**: 1623–1631.

589 50.   Shepherd PR, Gnudi L, Tozzo E, Yang H, Leach F, Kahn BB (1993) Adipose cell

590   hyperplasia and enhanced glucose disposal in transgenic mice overexpressing

591   GLUT4 selectively in adipose tissue. *J Biol Chem* **268**: 22243–22246.

592 51.   Beaven SW, Matveyenko A, Wroblewski K, Chao L, Wilpitz D, Hsu TW, Lentz J,

593   Drew B, Hevener AL, Tontonoz P (2013) *Reciprocal Regulation of Hepatic and*

594   *Adipose Lipogenesis by Liver X Receptors in Obesity and Insulin Resistance*.

595 52.   Abreu-Vieira G, Fischer AW, Mattsson C, de Jong JMA, Shabalina IG, Rydén M,

596   Laurencikiene J, Arner P, Cannon B, Nedergaard J, et al. (2015) Cidea improves

597   the metabolic profile through expansion of adipose tissue. *Nat Commun* **6**: 7433.

598 53.   Li P, Song Y, Zan W, Qin L, Han S, Jiang B, Dou H, Shao C, Gong Y (2017)

599   Lack of CUL4B in Adipocytes Promotes PPARγ-Mediated Adipose Tissue

600   Expansion and Insulin Sensitivity. *Diabetes* **66**: 300–313.

601 54.   Grünberg JR, Hoffmann JM, Hedjazifar S, Nerstedt A, Jenndahl L, Elvin J,

602   Castellot J, Wei L, Movérare-Skrtic S, Ohlsson C, et al. (2017) Overexpressing

603   the novel autocrine/endocrine adipokine WISP2 induces hyperplasia of the

604   heart, white and brown adipose tissues and prevents insulin resistance. *Sci Rep*

605   **7**: 43515.

606 55.   Hammarstedt A, Sopasakis VR, Gogg S, Jansson P-A, Smith U (2005) Improved

607   insulin sensitivity and adipose tissue dysregulation after short-term treatment

608   with pioglitazone in non-diabetic, insulin-resistant subjects. *Diabetologia* **48**: 96–

609   104.

610 56.   Long W, Hui Ju Z, Fan Z, Jing W, Qiong L (2014) The effect of recombinant

611   adeno-associated virus-adiponectin (rAAV2/1-Acrp30) on glycolipid

612   dysmetabolism and liver morphology in diabetic rats. *Gen Comp Endocrinol* **206**:

613   1–7.

614 57.   Shklyaev S, Aslanidi G, Tennant M, Prima V, Kohlbrenner E, Kroutov V,

615   Campbell-Thompson M, Crawford J, Shek EW, Scarpace PJ, et al. (2003)

616   Sustained peripheral expression of transgene adiponectin offsets the

617   development of diet-induced obesity in rats. *Proc Natl Acad Sci U S A* **100**:

618   14217–14222.

619 58.   Cnop M, Havel PJ, Utzschneider KM, Carr DB, Sinha MK, Boyko EJ, Retzlaff

620   BM, Knopp RH, Brunzell JD, Kahn SE (2003) Relationship of adiponectin to

621   body fat distribution, insulin sensitivity and plasma lipoproteins: evidence for

622   independent roles of age and sex. *Diabetologia* **46**: 459–469.

623 59.   Ma H, Gomez V, Lu L, Yang X, Wu X, Xiao SY (2009) Expression of adiponectin

624   and its receptors in livers of morbidly obese patients with non-alcoholic fatty liver

625   disease. *J Gastroenterol Hepatol* **24**: 233–237.

626 60.   Xu A, Wang Y, Keshaw H, Xu LY, Lam KSL, Cooper GJS (2003) The fat-derived

627   hormone adiponectin alleviates alcoholic and nonalcoholic fatty liver diseases in

628   mice. *J Clin Invest* **112**: 91–100.

629 61.   Ma H, Cui F, Dong J-J, You G-P, Yang X-J, Lu H-D, Huang Y-L (2014)

630   Therapeutic effects of globular adiponectin in diabetic rats with nonalcoholic fatty

631   liver disease. *World J Gastroenterol* **20**: 14950–14957.

632

FIGURE LEGENDS

634

635 **Figure 1. BMP7 increases fat mass and reduces white adipocyte size.**

636 Ob/ob mice were administered intra-eWAT with $1x10^{12}$ vg/mouse of AAV-BMP7

637 vectors at 11 weeks of age. Control ob/ob mice received $1x10^{12}$ vg of AAV-null

638 vectors. (**A**) AAV-derived BMP7 expression in epididymal (eWAT),

639 retroperitoneal (rWAT), mesenteric (mWAT) and inguinal (iWAT) white adipose

640 depots, interscapular BAT (iBAT) and the liver 3 months after AAV-treatment.

641 The qPCR was performed with primers that specifically detected the murine

642 optimized-BMP7 (moBMP7) coding sequence. n=7-10. (**B**) Circulating levels of

643 BMP7 3 months after vector administration. n=8-10. (**C**) Evolution of body

644 weight in animals treated with AAV-BMP7 or AAV-null vectors. n=8-10. (**D**)

645 Weight of several WAT and BAT depots and the liver in the same cohorts of

646 mice as in (C). n=8-10. (**E**) Representative images of the hematoxylin-eosin

647 staining of eWAT and iWAT sections. Scale bars: 100 µm. (**F**) Mean area of

648 white adipocytes in eWAT and iWAT. n=8-10 (eWAT) and n=4 (iWAT). All

649 values are expressed as mean±SEM. ND, non-detected. AU, arbitrary units.

650 **P<0.01 and ***P<0.001 versus the AAV-Null-treated group.

651

652 **Figure 2. BMP7 induces white adipogenesis and decreases WAT**

653 **inflammation.** (**A,B**) Expression of adipogenic markers in eWAT (A) and iWAT

654 (B). (**C,D**) Expression of markers of mature adipocytes in eWAT (C) and iWAT

655 (D). (**E**) Serum concentration of adiponectin. (**F**) Immunohistochemistry for the

656 macrophage-specific marker Mac2 in eWAT sections. Scale bars: 100 µm. (**G**)

657 Quantification by qRT-PCR of the expression levels of the macrophage markers

658   *Cd68* and *F4/80* in eWAT. (**H,I**) Expression of the pro-inflammatory markers

659   *Mcp1*(H) *and Tnfα* (I) in eWAT. All values are expressed as mean±SEM. *n*=8-

660   10. **P<0.01 and ***P<0.001 versus the AAV-null-injected group.

661

662   **Figure 3. WAT-derived BMP7 does neither induce brown adipogenesis nor**

663   **enhance non-shivering thermogenesis.** (**A**) Representative images of the

664   hematoxylin-eosin staining of iBAT sections of ob/ob mice treated intra-eWAT

665   with AAV-BMP7 or AAV-null vectors. Scale bars: 100 µm. (**B,C**) Quantification

666   by qRT-PCR of the expression levels of markers of adipogenesis (B) and of

667   mature adipocytes (C) in iBAT. *n*=7-10. (**D,E**) Quantification by qRT-PCR of the

668   expression of the thermogenic markers *Ucp1 and Ppargc1a* in iBAT (D) and

669   iWAT (E). *n*=7-9 (**F**) Energy expenditure was measured with an indirect open

670   circuit calorimeter 6 weeks after AAV vector delivery. *n*=8-9. Data were taken

671   during the light and dark cycles. All values are expressed as mean±SEM.

672

673   **Figure 4. BMP7 ameliorates hepatic steatosis.** (**A**) Representative images of

674   the hematoxylin-eosin staining of liver sections of ob/ob mice treated intra-

675   eWAT with AAV-BMP7 or AAV-null vectors. Scale bars: 200 µm and 50 µm

676   (inset). (**B**) Fed hepatic triglyceride content. *n*=8-10. (**C**) Immunostaining for the

677   macrophage-specific marker Mac-2 in liver sections. Red arrowheads indicate

678   Mac2^{+} cells. Scale bars: 100 µm and 50 µm (inset). (**D**) Quantification by qRT-

679   PCR of the expression of the macrophage marker *Cd68* in the liver. *n*=7-10. All

680   values are expressed as mean±SEM. **P<0.01 and ***P<0.001 versus the

681   AAV-null injected group.

682   **Figure 5. BMP7 improves insulin sensitivity.** (**A**) Fed blood glucose levels 3

683   months after vector administration. *n*=8-10. (**B**) Fed serum insulin levels 3

684   months after vector delivery. *n*=7-10. (**C**) Insulin tolerance test was performed

685   after an intraperitoneal injection of insulin (0.75 units/kg body weight) 2 months

686   post-AAV delivery. *n*=7-9. Results were calculated as the percentage of initial

687   blood glucose levels. All values are expressed as mean±SEM. *P<0.05 and

688   **P<0.01 versus the AAV-null injected group.

689

690   **Figure 6. Liver-derived BMP7 does not induce white adipogenesis.** Ob/ob

691   mice were administered intravenously with $5x10^{11}$ vg/mouse of AAV-hAAT-

692   BMP7 vectors at 11 weeks of age. Control ob/ob mice received $5x10^{11}$ vg of

693   AAV-hAAT-null vectors. (**A**) AAV-derived BMP7 expression in the liver, eWAT

694   and iWAT depots 5 months after AAV administration. Analysis by qPCR was

695   performed with primers that specifically detected the murine optimized-BMP7

696   (moBMP7) coding sequence. *n*=8-9. (**B**) BMP7 serum circulating levels 5

697   months after vector administration. *n*=7-9. (**C**) Body weight of animals treated

698   with either AAV-hAAT-BMP7 or AAV-hAAT-null vectors. *n*=8-9. (**D**) Weight of

699   the liver, epididymal (eWAT), inguinal (iWAT), retroperitoneal (rWAT) and

700   mesenteric (mWAT) white adipose tissue depots and interscapular brown

701   adipose tissue (iBAT). *n*=8-9. (**E**) Mean area of white adipocytes in eWAT and

702   iWAT. *n*=5. (**F**) Quantification by qRT-PCR of the expression levels of markers

703   of adipogenesis and of mature adipocytes in eWAT. *n*=7-9. (**G**) Serum levels of

704   adiponectin. *n*=8-9. (**H**) Immunohistochemistry for the macrophage-specific

705   marker Mac2 in sections of eWAT and liver. Scale bars: 100 μm and 50 μm

706   (inset). (**I,J**) Quantification by qRT-PCR of the expression of the macrophage

markers *Cd68* and *F4/80* in eWAT (I) and in the liver (J). *n*=7-9. (**K**) Fed hepatic

triglyceride content. *n*=8-9. (**L,M**) Fed blood glucose (L) and insulin (M) levels 5

months after vector administration. *n*=8-9. ND, non-detected. AU, arbitrary units.

All values are expressed as mean±SEM. **P*<0.05 versus the AAV-hAAT-null-

injected group.

SUPPLEMENTAL FIGURE LEGENDS

714

715 **Figure S1. Redistribution of the size of white adipocytes by WAT-derived**

716 **BMP7.** (**A**) Histogram depicting the food intake of ob/ob mice treated with

717 1×10^{12} vg/mouse of AAV-BMP7 or AAV-null vectors. n=8-10. (**B**) Activity was

718 measured 6 weeks after AAV vector delivery. n=8-9. Data were taken during the

719 light and dark cycles. (**C**) Frequency distribution of white adipocyte area in

720 eWAT of the same groups as in (A). n=8-10. All values are expressed as

721 mean±SEM.

722

723 **Figure S2. Liver-derived BMP7 failed to induce adipogenesis and did not**

724 **decrease hepatic steatosis.** (**A,B**) Representative images of the hematoxylin-

725 eosin staining of eWAT (A) and iWAT (B) sections of ob/ob mice treated

726 intravenously with 5×10^{11} vg/mouse of AAV-hAAT-BMP7 or AAV-hAAT-null

727 vectors. Scale bars: 100 μm. (**C**) Expression levels of adipogenic markers in

728 iWAT. n=7-9. (**D**) Representative images of hematoxylin-eosin staining of iBAT

729 sections. Scale bars: 100 μm. (**E**) Expression of markers of adipogenesis and of

730 mature adipocyte markers in iBAT. n=7-9. (**F,G**) Expression of markers of

731 thermogenesis in iWAT (F) and iBAT (G). n=7-9. (**H**) Representative images of

732 hematoxylin-eosin staining of liver sections. Scale bars: 200 μm and 50 μm

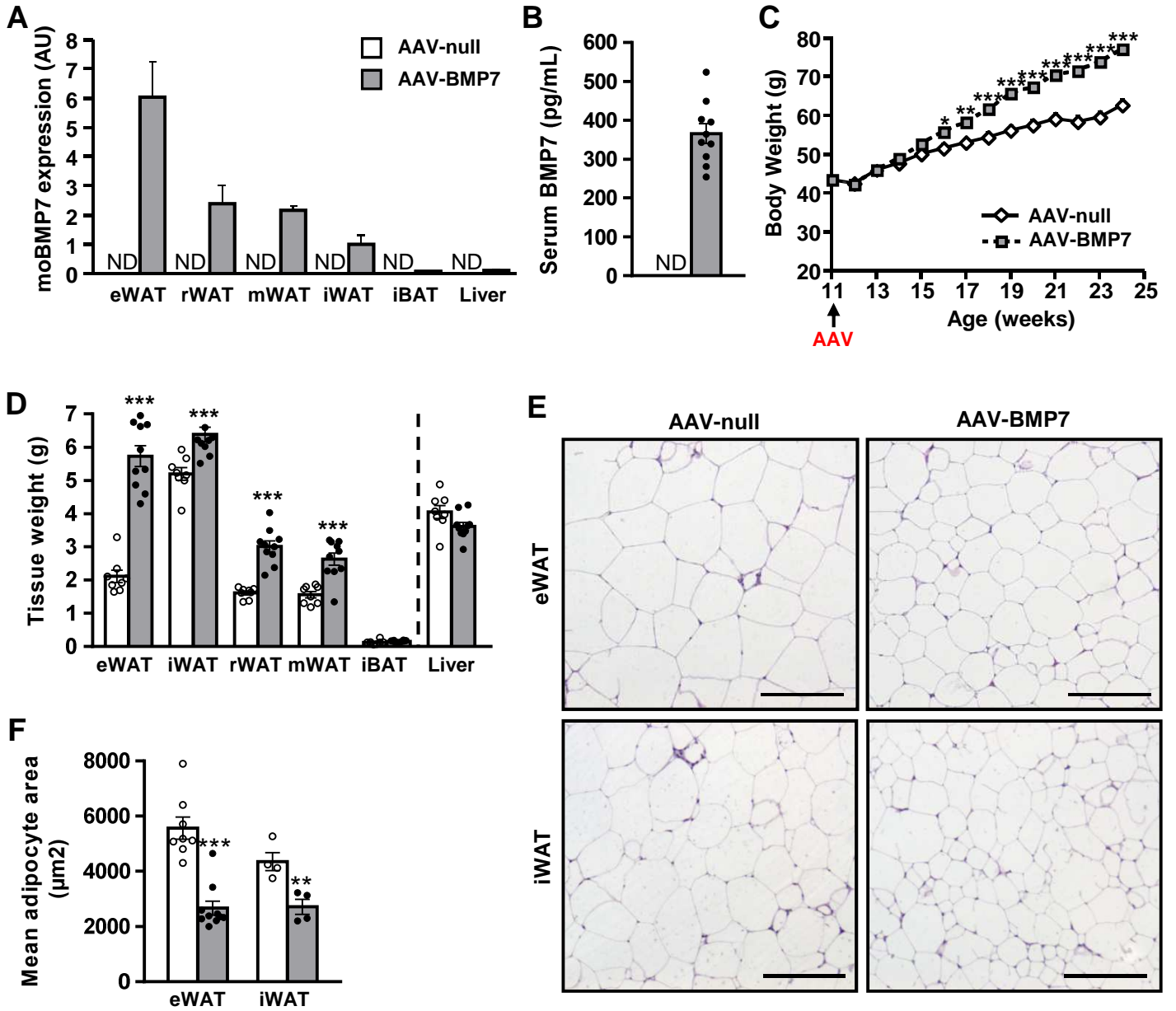733 (inset). All values are expressed as mean±SEM.

FIGURE 1

FIGURE 2

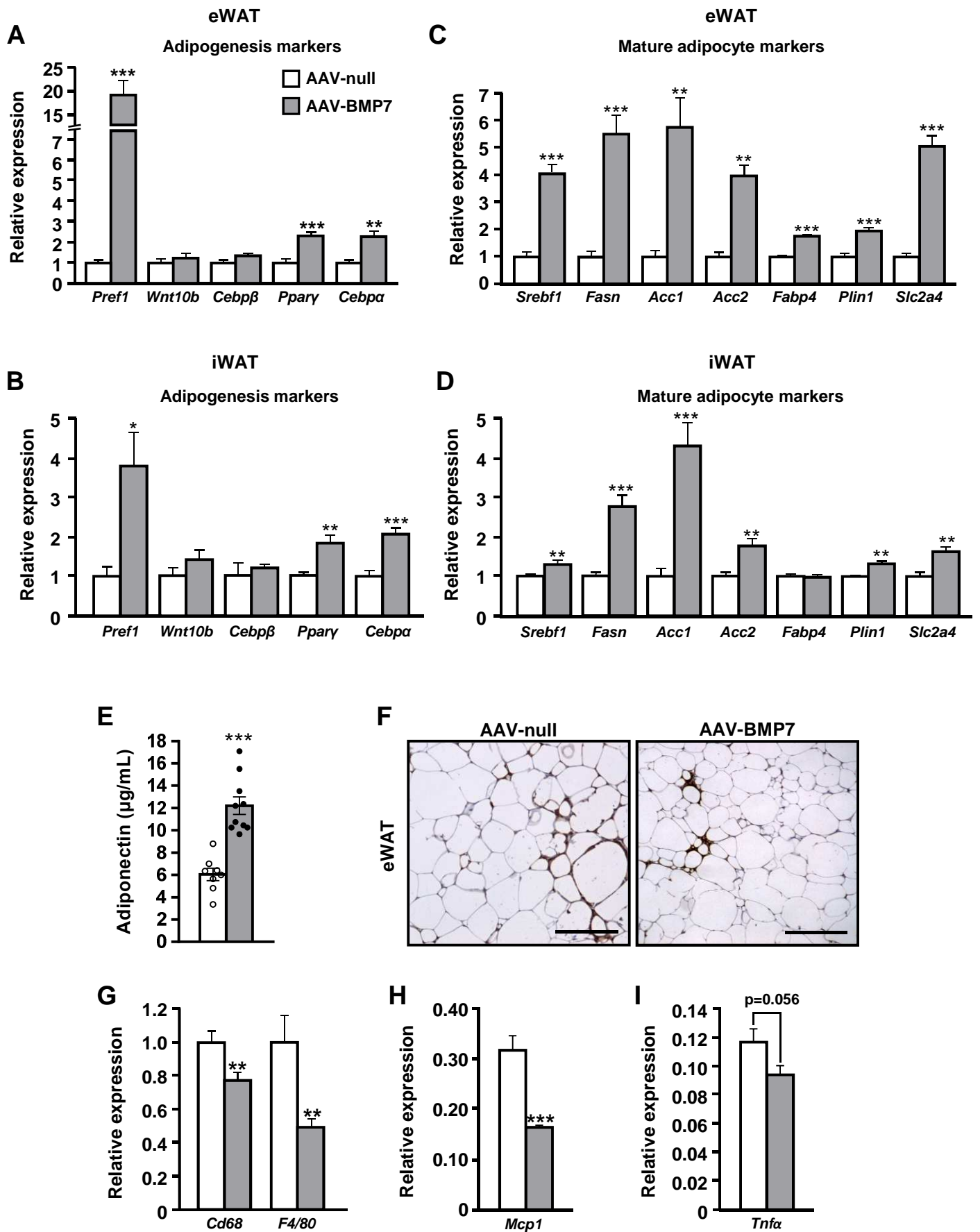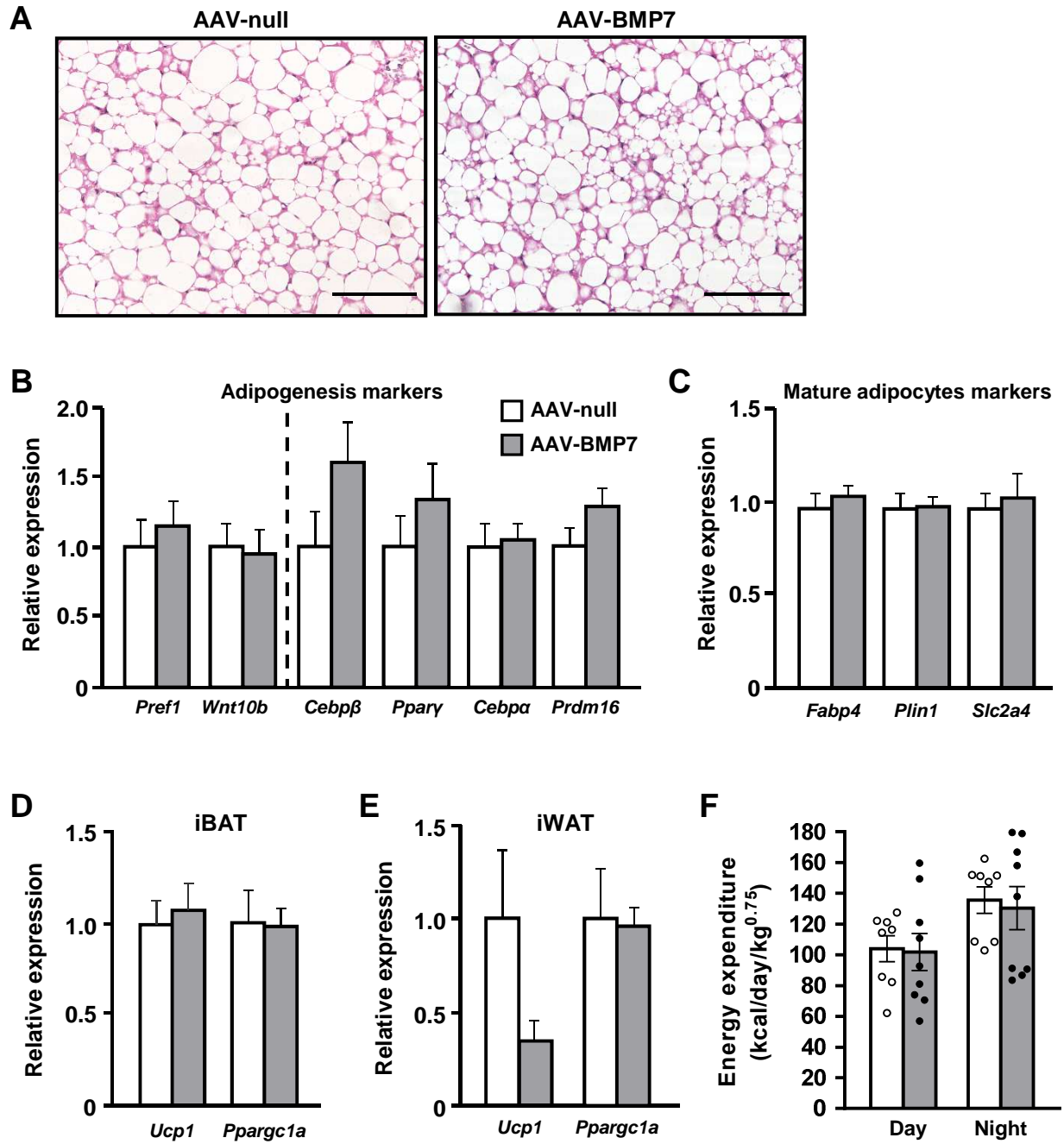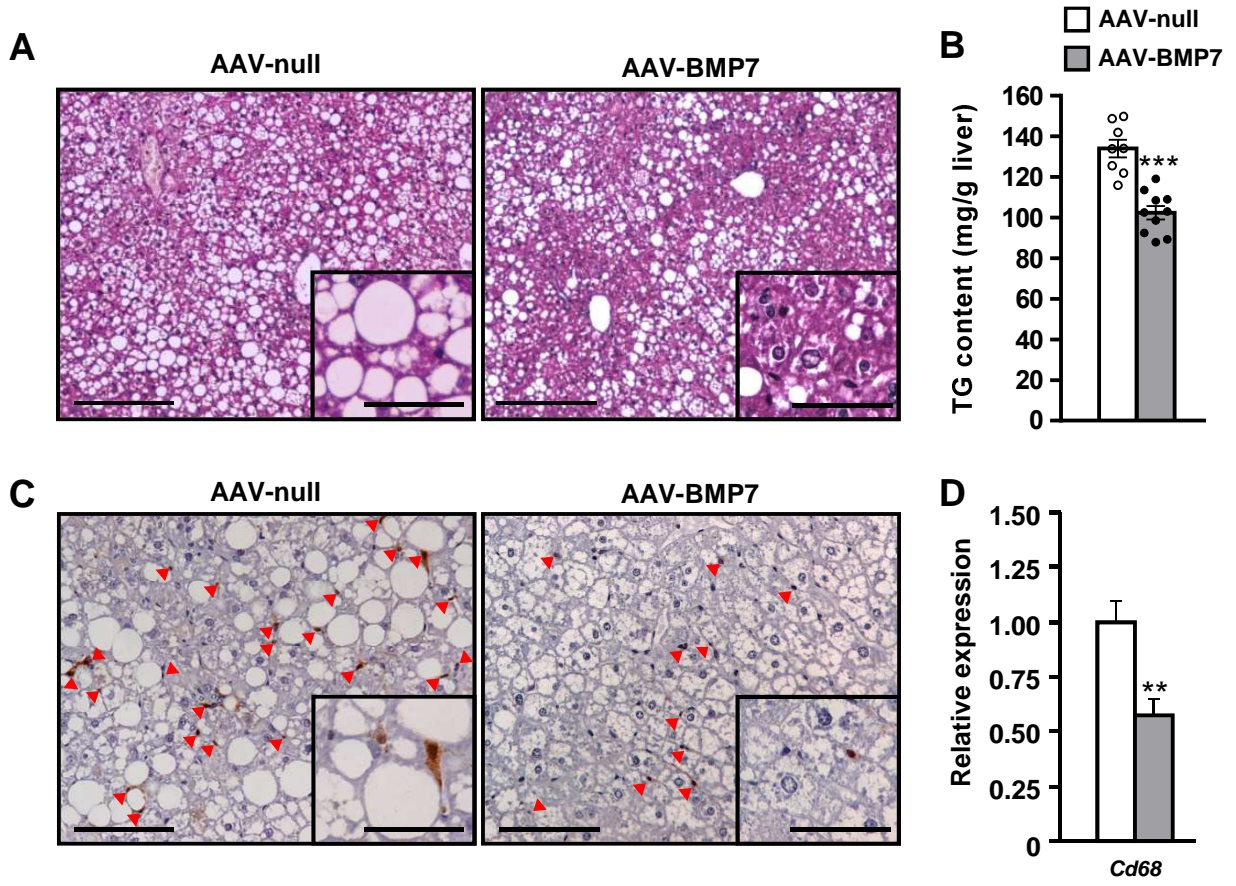**FIGURE 3**

A

AAV-null   AAV-BMP7

B   Adipogenesis markers

□ AAV-null
■ AAV-BMP7

Relative expression

Pref1   *Wnt10b*   *Cebpβ*   *Pparγ*   *Cebpα*   *Prdm16*

C   Mature adipocytes markers

Relative expression

Fabp4   *Plin1*   *Slc2a4*

D   iBAT

Relative expression

Ucp1   *Ppargc1a*

E   iWAT

Relative expression

Ucp1   *Ppargc1a*

F

Energy expenditure
(kcal/day/kg$^{0.75}$)

Day   Night

FIGURE 4

FIGURE 5

FIGURE 6